

Original Research

ANK3 Is Regulated by Recursive Splicing and Inhibits Hepatocellular Carcinoma Metastasis by Inhibiting E-Cadherin Protein Degradation

Yuanyuan Guo¹, Xianghui Fu¹, Yan Tian^{1,*}

¹Department of Biotherapy, State Key Laboratory of Biotherapy, West China Hospital, Sichuan University, 610041 Chengdu, Sichuan, China

Academic Editor: Seok-Geun Lee

Submitted: 24 August 2025 Revised: 26 September 2025 Accepted: 11 October 2025 Published: 30 October 2025

Abstract

Background: Ankyrin G (ANK3), belonging to the ankyrin family, contributes to cellular structural integrity by linking the cytoskeleton to the plasma membrane. Abnormal ANK3 expression has been reported across several human malignancies, yet the regulatory mechanisms involved are still poorly understood. The process of dividing introns into several steps is referred to as recursive splicing (RS). RS can control the quality of transcripts produced by regulating the retention of the RS-exon. Hundreds of annotated RS-exons in human mRNAs are attributed to the inhibition of RS by the exon junction complex (EJC). Methods: In this study, we demonstrated that ANK3 is reduced in hepatocellular carcinoma (HCC) and suppresses HCC metastasis. We then analyzed the multiple splicing methods of ANK3, confirming that RS exists in ANK3 transcript variant 4 (ANK3-TV4) and that RS was weakened in HCC. Results: Mechanistically, ANK3 inhibited HCC metastasis, which may be partly attributed to inhibition of the Wnt pathway. ANK3 binds to E-cadherin via its N-terminal ankyrin repeat domain to regulate E-cadherin expression. ANK3 knockdown activates the Wnt pathway, downregulates E-cadherin expression, and promotes its degradation. Conversely, ANK3-TV4 overexpression inhibited the Wnt signaling pathway, upregulated E-cadherin protein expression, and inhibited E-cadherin degradation. RBM8A, a core EJC factor, regulates the RS of ANK3-TV4. Conclusions: Knockdown of RBM8A promoted RS of ANK3-TV4 and upregulated its expression. We investigate the role of RS in HCC, providing a novel therapeutic perspective and identifying potential targets for intervention.

Keywords: ankyrin G; recursive splicing; hepatocellular carcinoma

1. Introduction

Liver cancer ranks as the sixth most prevalent malignancy globally and is the third leading cause of cancer-related mortality [1]. Hepatocellular carcinoma (HCC) constitutes nearly 80% of primary liver cancer cases [2]. Patients with HCC generally face poor clinical outcomes and limited effective treatment options [3]. Therefore, elucidating the pathogenic mechanism of HCC and its key regulatory molecules is essential for developing novel therapeutic strategies aimed at its prevention and treatment. Several studies have highlighted alternative splicing (AS) as an important source of new prognostic biomarkers and therapies for HCC [4–10].

More than 90 percent of human genes generate different transcripts through AS, thereby forming diversified transmissions of genetic information [5,11–14]. Recursive splicing (RS) is a noncanonical splicing mechanism in which introns are cut in several steps. In general, an RS-exon exists in the introns of genes that produce RS. This exon contains a premature termination codon (PTC), which commonly activates the nonsense-mediated mRNA decay (NMD) and terminates translation. RS removes the RS-exon, which can prevent the production of abnormal N-terminal mutant or truncated proteins, thereby maintaining normal gene expression and cellular functions [15,16]. Several studies have shown that the Exon Junction Complex

(EJC) suppresses RS and is an important factor in abnormal RS [17,18]. It is worth emphasizing that, as a rare AS pattern, RS has seldom been studied; moreover, its underlying mechanisms and implications in cancer remain poorly understood.

Cytoskeletal rearrangement is necessary for multiple pathological processes, such as the migration and invasion of tumor cells, and plays a key role in tumor metastasis [19]. Therefore, in-depth research on this topic is of great significance for identifying the intrinsic mechanisms and targets of tumor metastasis and developing new targeted therapies. Ankyrin 3 (ANK3), a member of the Ankyrin family, plays a crucial role in maintaining cell stability by linking the cytoskeleton to the plasma membrane [20,21]. ANK3 typically comprises three major functional regions: an Nterminal membrane-interacting domain, a central domain that engages pectin/fodrin, and a regulatory C-terminal domain [20,22]. Current studies have reported that there are multiple transcripts of ANK3 [16,23,24] and it is abnormally expressed across various tumor types [21]. Nonetheless, the association between ANK3 expression and AS in HCC patients has not yet been elucidated.

In our study, we first demonstrated that *ANK3* was downregulated in HCC and inhibited HCC metastasis, confirming that RS exists in *ANK3* transcript variant 4 (*ANK3-TV4*) and that RS is weakened in HCC. Mechanistically,

^{*}Correspondence: tyfxh@163.com (Yan Tian)

ANK3 inhibited HCC metastasis, which may be partly attributed to inhibition of the Wnt pathway. *ANK3* binds to Ecadherin via its N-terminal ankyrin repeat domain to regulate E-cadherin expression. *ANK3* knockdown activates the Wnt pathway, downregulates E-cadherin expression, and promotes its degradation. Conversely, overexpression of *ANK3-TV4* had opposite effects. *RBM8A*, a core EJC factor, regulates the RS of *ANK3-TV4*. *RBM8A* knockdown promotes the RS of *ANK3-TV4*. We explored the involvement of RS in HCC, offering a new strategy for HCC treatment and identifying promising targets.

2. Materials and Methods

2.1 Cell Culture

SNU449, SK-Hep1, and Huh7 cells were purchased from the Type Culture Cell Bank of the Chinese Academy of Sciences (Shanghai, China). Cells were cultured following the protocols provided by the supplier. All the cells in this study were purchased from the Type Culture Cell Bank of the Chinese Academy of Sciences (Shanghai, China). All cell lines were validated by STR profiling and tested negative for mycoplasma.

2.2 Transfection

Small interfering RNAs (siRNAs) used in this study were commercially synthesized by GenePharma (Shanghai, China). Transfection was carried out using HiPerfect for siRNAs and Attractene for plasmids (Qiagen, Hilden, Germany), as per the supplier's guidelines. Details of the siRNA sequences can be found in **Supplementary Table 1**.

2.3 RNA Extraction and PCR (Including RT-PCR and aRT-PCR)

Total RNA was isolated using Tri-Reagent (Molecular Research Center, Cincinnati, OH, USA) following the manufacturer's standard protocol. We performed RT-PCR by first generating cDNA with the TransScript One-Step gDNA Removal and cDNA Synthesis SuperMix (TRAN, Beijing, China). The subsequent amplification step utilized the Golden Star T6 Super PCR Mix (TSINGKE, Beijing, China), as per the manufacturer's instructions. Primer sequences are listed in **Supplementary Table 2**.

cDNA synthesis for real-time quantitative PCR (qRT-PCR) was carried out using murine leukemia virus reverse transcriptase (Invitrogen, Life Technologies, Carlsbad, CA, USA), followed by amplification with Power SYBR Green PCR Master Mix (Applied Biosystems, Foster City, CA, USA). Gene expression levels were normalized to β -actin, with corresponding primer sequences shown in **Supplementary Tables 3,4**.

2.4 Cell Proliferation

To assess cell proliferation, an 3-[4,5-dimethylthiazol-2-yl]-5-[3-carboxymethoxyphenyl]-2-[4-sulfophenyl]-2H-

tetrazolium (MTS) assay was performed according to the established method [25]. Briefly, 2500 cells were inoculated in a 96-well plate, and cell proliferation rates were measured using the CellTiter 96 AQ Ueous Nonradioactive Cell Proliferation Assay (MTS) (Promega, Madison, WI, USA) according to the manufacturer's instructions [26].

2.5 Lentivirus Transduction

To knock down ANK3 or RBM8A, we utilized the pLKO.1 lentivirus vector (Addgene, Cambridge, Massachusetts, USA). Target cells were transduced with viral particles in the presence of polybrene (2 mg/mL; Sigma-Aldrich, St. Louis, MO, USA), and puromycin (Sigma-Aldrich) was applied for the selection of positive cells. Refer to **Supplementary Table 1** for the short hairpin RNAs (shRNAs) sequences.

2.6 Cell Migration and Invasion Experiment

Cell migration and invasion experiments were performed as described previously [25]. For the woundhealing experiment, cells were cultured in 6-well plates to achieve a confluent monolayer. A sterile pipette tip was used to induce scratches. Cell migration into the scratch area was then monitored and photographed. To assess cell migration and invasion, transwell assays were performed. 5×10^4 cells per well in serum-free medium were plated in the upper chamber. For the invasion assay, the membrane was pre-coated with a substrate matrix, while it was left uncoated for migration. Following a 24-hour incubation, cells on the lower membrane surface were stained with crystal violet for microscopic observation [26].

2.7 Immunoblotting

Western blot analysis was performed on total protein extracts using standard protocols [27]. Respective primary antibodies against E-Cadherin (1:1000, 3195, Cell Signaling Technology, Danvers, MA, USA), β -Catenin (1:1000, 9562, Cell Signaling Technology, Danvers, MA, USA), β -actin (1:1000, 20536-1-AP, Proteintech, Wuhan, China), β -Tubulin (1:1000, 10094-1-AP, Proteintech, Wuhan, China), glyceraldehyde-3-phosphate dehydrogenase (GAPDH) (1:1000, 10494, Proteintech, Wuhan, China), and ANK3 (1:1000, 27980-AP, Proteintech, Wuhan, China) were utilized for detection.

2.8 Histology and Immunostaining

We performed immunohistochemical (IHC) staining on formalin-fixed, paraffin-embedded tissue sections. The sections were incubated with an anti-ANK3 antibody (1:2000, 27980-AP, Proteintech, Wuhan, China) following the manufacturer's instructions.

2.9 Human Liver Samples

Paired clinical specimens, comprising liver tumors and their matched adjacent normal tissues, were obtained



from West China Hospital of Sichuan University. Total RNA was extracted from these tissues with Tri-Reagent and subsequently analyzed via qRT-PCR. This study obtained ethical approval from the Ethics Committee of West China Hospital of Sichuan University (2020, no. 196) for the use of human samples. All participants provided written informed consent prior to inclusion.

2.10 Statistical Analysis

Data are presented as mean \pm SEM from a minimum of three independent replicates. The threshold for statistical significance was set at p < 0.05, marked by asterisks (Nonsignificant (NS) for p > 0.05, * for p < 0.05, ** for p < 0.01, and *** for p < 0.001). Group comparisons were conducted using two-way ANOVA, Student's t-test, or paired t-test, as applicable.

3. Results

3.1 ANK3 is Downregulated in HCC and Inhibits the Migration and Invasion of HCC Cells In Vitro

To elucidate the role of ANK3 in HCC, we used GSE20017 data from the NCBI to analyze the expression of ANK3, and found that ANK3 expression in patients with microvascular invasion was markedly lower than that in patients without microvascular invasion (Fig. 1a), suggesting that ANK3 may be involved in regulating HCC metastasis. We investigated ANK3 expression in human HCC tissues. ANK3-total mRNA levels were lower in HCC tissues (Fig. 1b), consistent with publicly available data (Fig. 1c). Western blot (WB) results showed that the patterns of the different sizes of ANK3 proteins were inconsistent. The protein, approximately 150 kDa (ANK3-TV2), was significantly downregulated in HCC tissues, while the expression pattern of the protein, approximately 250 kDa (ANK3-TV3/4/5), was uncertain (Fig. 1d). IHC analysis further confirmed reduced ANK3 levels in HCC samples (Fig. 1e).

We next assessed whether *ANK3* contributes to liver tumorigenesis. *ANK3* knockdown by siRNA had no impact on the growth of SNU449 or SK-Hep1 cells (**Supplementary Fig. 1**), indicating that *ANK3* does not regulate HCC proliferation. Conversely, *ANK3* knockdown markedly promoted the migration ability of SNU449 and SK-Hep1 cells (Fig. 1f,g), which was confirmed by a wound-healing experiment (Fig. 1h). Collectively, these *in vitro* findings establish that *ANK3* functions primarily to suppress the migratory and invasive capabilities of HCC cells.

3.2 Recursive Splicing of ANK3-TV4 Exists in Human Liver Tissue

With reference to NCBI, we analyzed the splicing methods existing in *ANK3* (Fig. 2a), including alternative promoters and exon jumping, which resulted in *ANK3* producing five transcripts. The five transcriptional variants (TVs) of human *ANK3* in the NCBI

database encoded three proteins of different sizes. First, through an alternative promoter, ANK3 produces four transcription start sites that produce four transcripts: transcript variant 3 (TV3) (NM 001204403), transcript variant 4 (TV4) (NM 001204404), transcript variant 1 (TV1) (NM_020987), and transcript variant 2 (TV2) (NM_001149). As a result of exon jumping, TV1 produces another transcription variant named transcript variant 5 (TV5) (NM 001320874), which lacks exon 37. Another study reported that TVI also underwent alternative 5' splicing and retained a part of exon 37 [28]. In addition, RS has been reported in ANK3 [16]. Sequence alignment and analysis revealed that RS may exist in ANK3-TV4. We first used primers from the literature for RT-PCR [16] but failed to detect RS-exon in human liver tissue. We then redesigned the primers and performed a nested PCR. Primer a was used for the first round of PCR, b/c/d/e primers were used for the second round of PCR in lanes 1/2/3/4, respectively (Fig. 2b,c). Theoretically, there were two bands in lane 1 at 103 bp (RS exon skipping) and 255 bp (RS exon retention). However, in lane 1, only the 103 bp band was visible to the naked eye, suggesting that only a small proportion of transcripts retained the RS-exon. The product sizes in lanes 2 and 3 (using primers c and d, respectively) were the same as expected. Collectively, our results demonstrate that the RS and RS-exon exist in ANK3-TV4 in the human liver and hepatoma tissues.

3.3 RS of ANK3-TV4 is Weakened in HCC, and ANK3-TV4 Suppresses the Migration and Invasion of HCC In Vitro

As illustrated in Fig. 1, *ANK3* expression was markedly reduced in HCC. We designed primers specific to different *ANK3* transcripts to detect their expression in human HCC tissues. All transcripts were significantly downregulated in HCC (Fig. 2d), which was consistent with the publicly available data (Fig. 2e,f). In addition, the results showed that in *ANK3-TV4*, the transcript with RS-exon skipping was significantly downregulated in HCC (Fig. 3a,b), whereas the transcript with RS-exon retention showed no significant pattern (Fig. 3c). Similar results were obtained by semi-quantitative PCR (Fig. 3d). This suggests that the RS of *ANK3-TV4* was weakened in HCC.

Next, we explored the role of *ANK3-TV4* in liver tumorigenesis. Because of the particularity of the *ANK3-TV4* sequence, only one pair of siRNAs could be specifically designed. Specific knockdown of *ANK3-TV4* by siRNAs markedly promoted the migration ability of SNU449 cells, as demonstrated by transwell and invasion assays as well as a wound-healing assay (Fig. 3e,f), suggesting that cell migration and invasion are suppressed by *ANK3-TV4* in vitro.

3.4 ANK3 Significantly Inhibits HCC Metastasis Through its Ankyrin Repeat Domain

Structurally, *ANK3* is organized into three functional domains: the N-terminal membrane domain (including



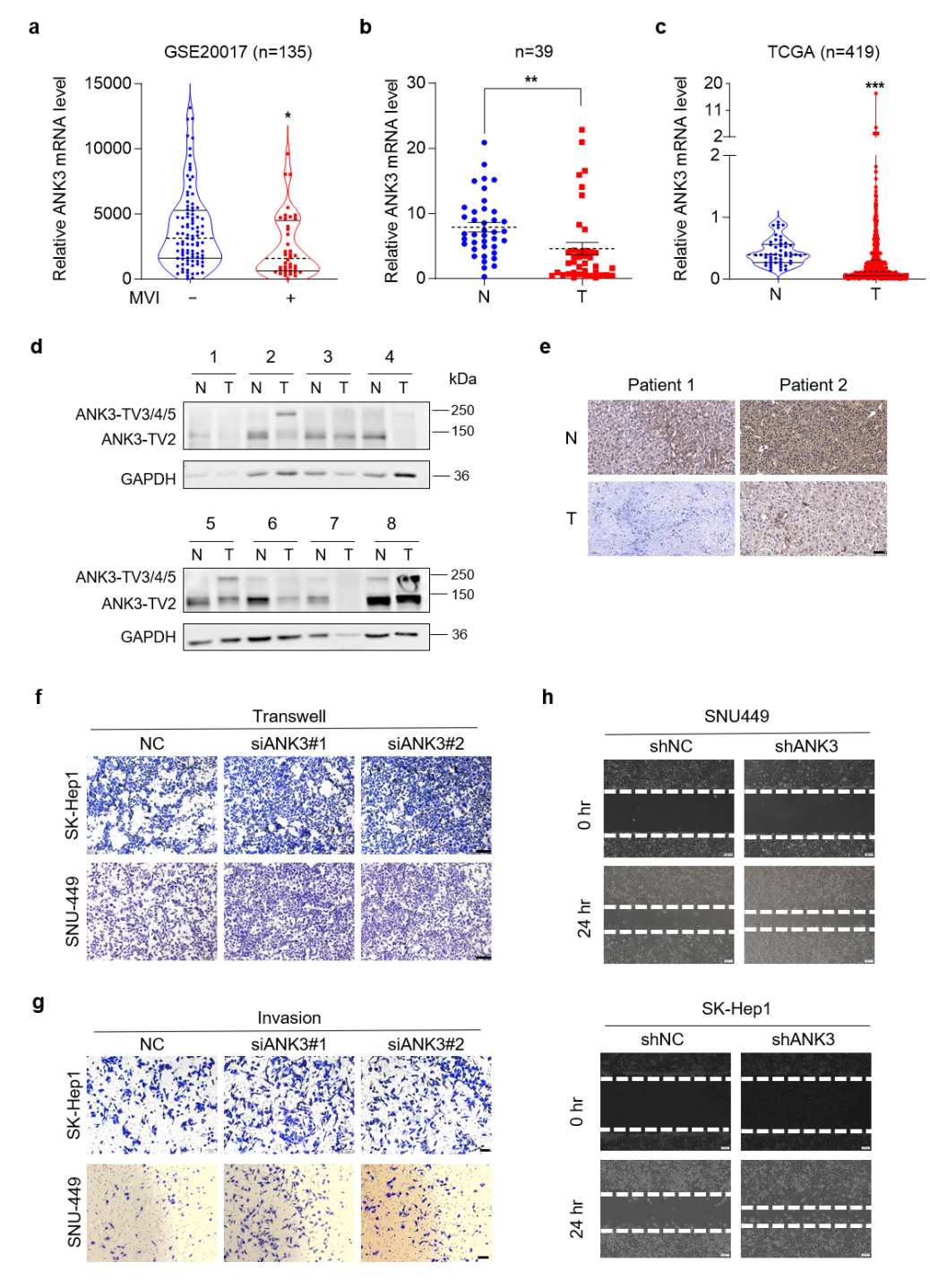


Fig. 1. Ankyrin 3 (*ANK3*) is significantly down-regulated in hepatocellular carcinoma (HCC). Knockdown of *ANK3* promotes HCC metastasis. (a) Dot plots depicting *ANK3* expression in HCC patients stratified by microvascular invasion (MVI) status (GSE20017 dataset). (b) Total *ANK3* mRNA levels in 39 paired HCC (T) and adjacent non-tumorous (N) tissues. (c) *ANK3* expression levels in HCC (T) and adjacent non-tumorous (N) tissues from the The Cancer Genome Atlas (TCGA) cohort. (d) Representative western blot (WB) images of *ANK3* protein in 8 paired HCC (T) and adjacent non-tumor (N) samples, with quantitative analysis relative to Glyceraldehyde-3-phosphate dehydrogenase (GAPDH) shown below. (e) IHC staining of *ANK3* in representative HCC and matched adjacent tissue. (f) Transwell assay of SK-Hep1 (top) and SNU449 (bottom) cells transfected with negative control (NC) or siANK3. (g) Invasion assay of SK-Hep1 (top) and SNU449 (bottom) cells transfected with NC or siANK3. (h) Wound-healing assay of SNU449 (top) and SK-Hep1 (bottom) cells transfected with shNC or ANK3 shRNA (shANK3). Scale bar: 50 μm (e), 100 μm (f,g), 200 μm (h). Data are presented as mean \pm SEM, *p < 0.05, **p < 0.01, ***p < 0.001 (Student's paired t test).

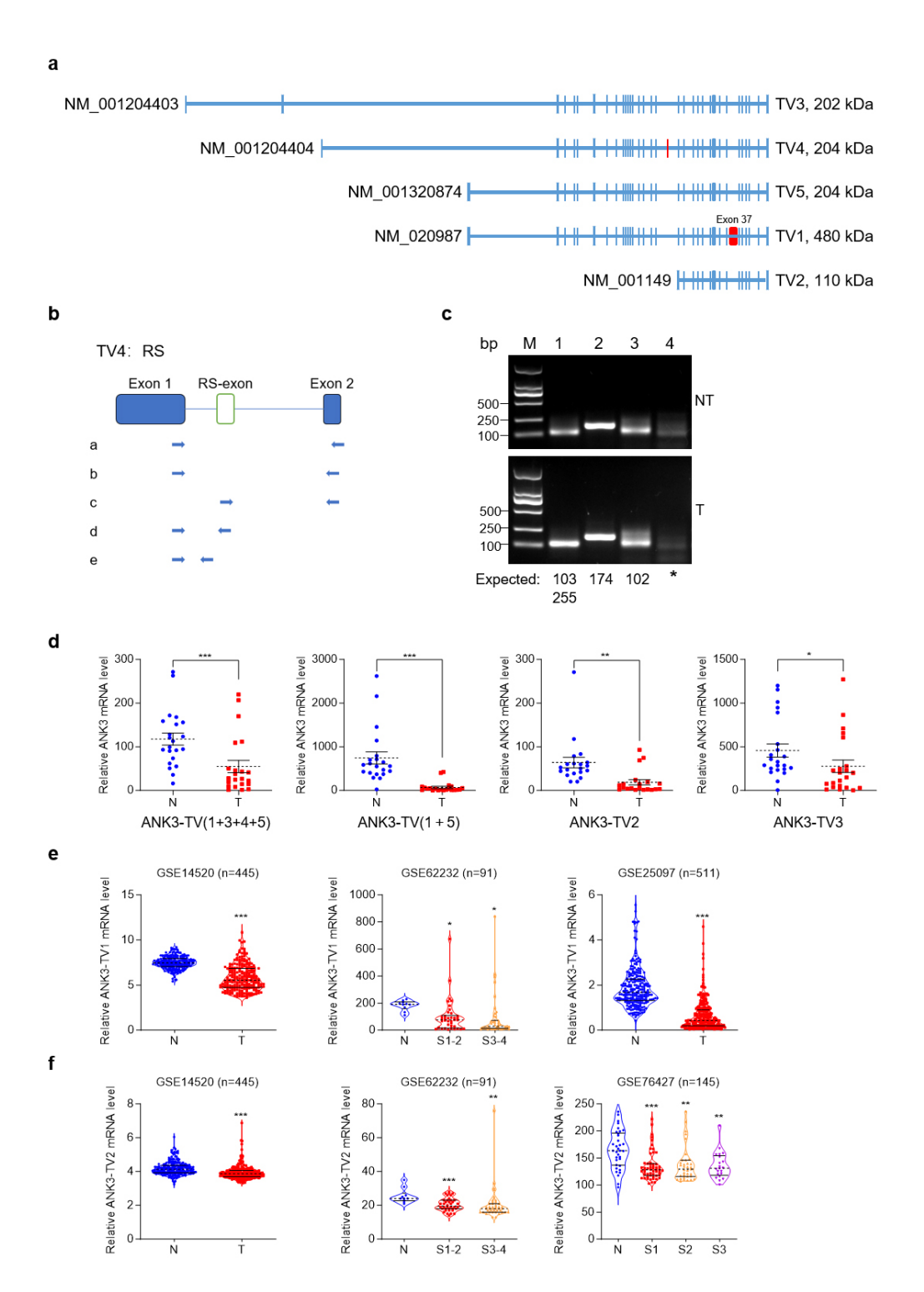


Fig. 2. Transcriptome structure diagram of *ANK3*. *ANK3* transcript variant 4 (TV4) undergoes recursive splicing (RS). (a) ANK3 from the NCBI database underwent alternative promoter and exon jumps, producing five TVs. The blue boxes represent exons. The red boxes represent the unique exons of TVI and TV4, respectively. (b) Schematic diagram of the nested PCR primers. (c) ANK3-TV4 undergoes RS. Using the nest-PCR assay, ANK3-TV4 was recursively spliced in both HCC tumours (T, down) and adjacent non-tumor (NT, up). Primer a was used for the first round of PCR. b/c/d/e primers were used for the second round of PCR in lanes 1/2/3/4, respectively. PCR product sizes are annotated below each lane. (d) mRNA levels of different transcripts in T and N tissues. (e) mRNA level of ANK3-TV1 in available HCC databases. (f) mRNA level of ANK3-TV2 in available HCC databases. Data are presented as mean \pm SEM, *p < 0.05, **p < 0.01, **p < 0.001 (Student's paired t test).

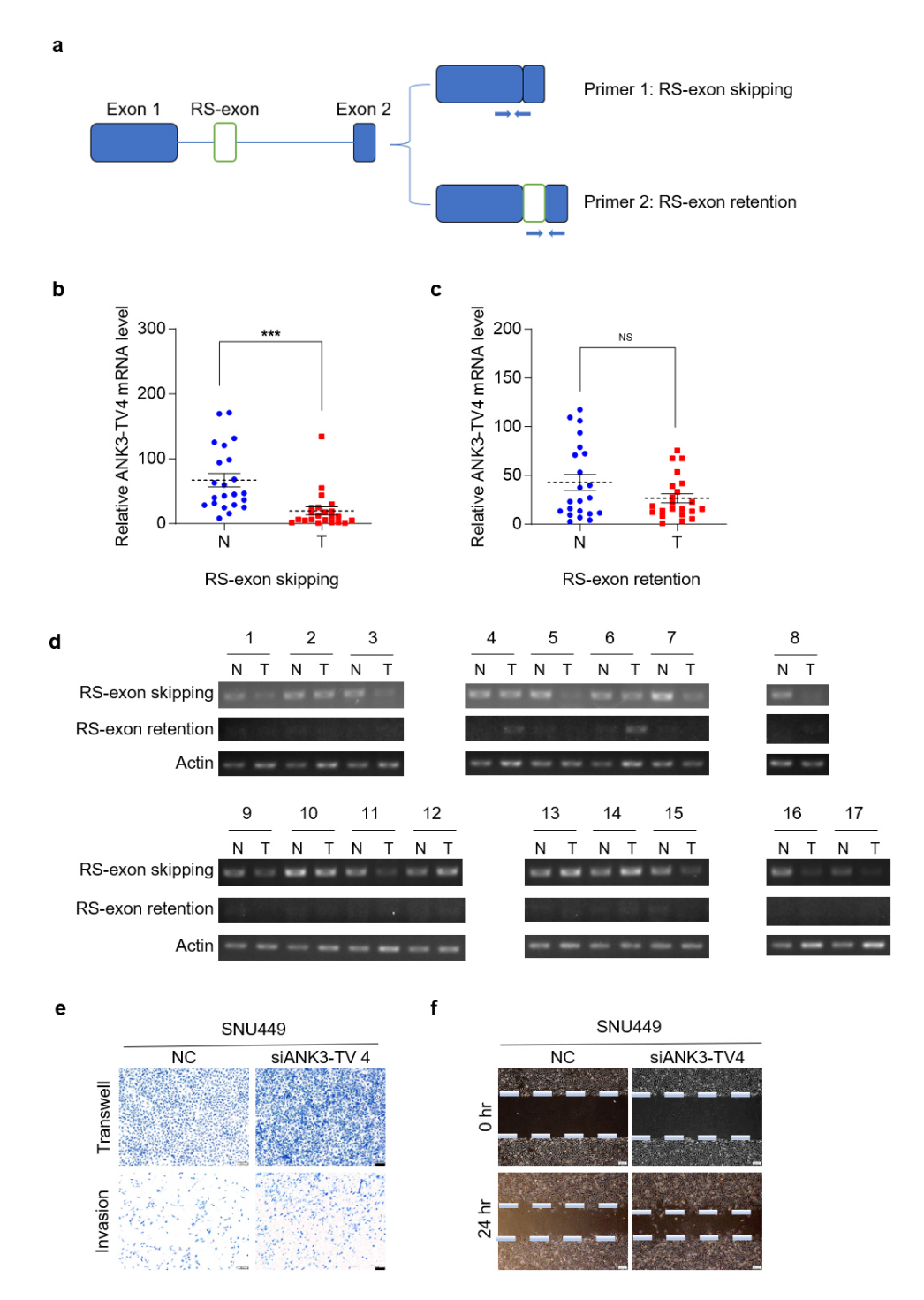


Fig. 3. RS of *ANK3-TV4* is weakened in HCC, and *ANK3-TV4* inhibits the metastasis of HCC cells. (a) Primer 1 was designed across the primary/secondary exon of *ANK3-TV4*, specifically quantifying the transcripts with RS (RS-exon skipping). Primer 2 was designed in the *ANK3-TV4* RS-exon and the second exon, respectively, specifically quantifying the transcripts with RS-exon retention. (b) Quantification of *ANK3-TV4* (RS-exon skipping) mRNA in HCC (T) and paired non-cancerous tissues (N). (c) mRNA abundance of *ANK3-TV4* (RS-exon retention) in HCC samples (T) relative to adjacent controls (N). (d) Semi-quantitative PCR analysis of both ANK3-TV4 splicing variants in 24 clinical sample pairs (Cycle parameters: Actin-25, *ANK3-TV4*-40). (e) Transwell and invasion assays of SNU449 cells following *ANK3-TV4* knockdown. (f) Wound-healing assay of SNU449 cells transfected with NC or siANK3-TV4. Scale bar: 100 μm (e), 200 μm (f). Data are presented as mean \pm SEM, NS: p > 0.05, ***p < 0.001 (Student's paired t test).

24 anchoring protein repeat sequences responsible for binding the entire membrane protein), a central spectrum protein/fodrin-binding domain that connects the anchoring protein to the actin-based cytoskeleton through spectrum



protein isomers, and a C-terminal regulatory domain [20]. All other transcripts contained the three domains, except for ANK3-TV2, which completely lacked the ankyrin repeat domain. To explore the influence of various ANK3 domains on HCC migration, ANK3-TV2 was initially overexpressed in stable ANK3-total knockdown cells to assess its impact on metastatic behavior. Overexpression of ANK3-TV2 did not markedly restore the promoting effect of ANK3 knockdown on cell migration (Fig. 4a,b). Since ANK3-TV2 lacks while ANK3-TV4 contains an ankyrin repeat domain, we compared the effects of overexpressing ANK3-TV2 and the ankyrin repeat-containing ANK3-TV4 (Supplementary Fig. 2a-c). The results clearly showed that only ANK3-TV4 significantly inhibited HCC cell invasion and migration (Fig. 4c-e), suggesting that ANK3 significantly inhibits HCC metastasis through its ankyrin repeat domain.

3.5 Knocking Down ANK3 Activates the Wnt Pathway and Promotes E-cadherin Protein Degradation

To explore the molecular mechanism of ANK3 regulation of cell migration, transcriptomic sequencing was performed on RNA extracted from stable ANK3 knockdown SNU449 cells. Gene Ontology Enrichment Analysis (GO) showed that ANK3 participates in the regulation of the Wnt signaling pathway (Fig. 5a-d). We initially searched for proteins that might interact with ANK3 in the BioGrid database and found that ANK3 might interact with 151 proteins (Supplementary Fig. 3a). We screened the proteins associated with metastasis and summarized them in Supplementary Fig. 3b. At the same time, we reviewed the literature on these proteins. E-cadherin, located in the cytomembrane, has been reported to interact with ANK3 and β -catenin in the cytoplasm to form ternary complexes. ANK3 knockdown facilitates the dissociation of β catenin from E-cadherin, and its subsequent translocation into the nucleus, thereby activating the canonical Wnt signaling pathway [29].

Based on the transcriptome sequencing results, BioGrid database search, and literature review, we selected E-cadherin as the research object and conducted subsequent experimental verification. The schematic diagram of the ANK3 domain is shown in Fig. 6a. The expression of HA-tagged control and E-cadherin plasmid in 293T cells is shown in Fig. 6b. Western Blot assay showed that the E-cadherin antibody could precipitate ANK3 containing an ankyrin repeat domain with a size of approximately 240 kDa and E-cadherin, but could not precipitate ANK3-TV2 lacking the ankyrin repeat domain with a size of 110 kDa (Fig. 6c), indicating that endogenous Ecadherin interacts with the ankyrin repeat domain of ANK3. A co-immunoprecipitation (Co-IP) assay confirmed that ANK3-TV4 could, while ANK3-TV2 couldn't, interact with E-cadherin (Fig. 6d,e). ANK3-TV4 overexpression significantly upregulated E-cadherin expression in Huh7 cells (Fig. 6f).

Transcriptomic sequencing suggests that knockdown of *ANK3* can activate the Wnt pathway. We first examined the potential role of *ANK3* in regulating the Wnt signaling pathway. Both qPCR and WB experiments confirmed that *ANK3* knockdown significantly upregulated the expression of several Wnt pathway components (Fig. 7a), while *ANK3-TV4* overexpression inhibited the expression of these genes (Fig. 7b).

The pro-metastatic function of Wnt/ β -catenin signaling is well-established across multiple cancer types and is attributed to the unique transcriptional program induced by the β -catenin/TCF complex [30]. Within this pathway, the TCF/LEF family transcription factor TCF4 (also known as TCF7L2) plays a pivotal role. Utilizing its HMG domain for DNA binding, TCF4 activates the expression of Wnt target genes, a function shared across the four members of the TCF/LEF family (TCF1, TCF3, TCF4, and LEF) [31]. In stable ANK3-total knockdown cells, TCF4 and β -catenin were knocked down instantaneously, both of which could restore the promoting effect of ANK3 knockdown on cell migration (Fig. 7c–f). These data suggested that ANK3 participates in HCC progression by influencing the Wnt pathway.

ANK3 binds to E-cadherin via its N-terminal ankyrin repeat domain to regulate E-cadherin expression. ANK3 knockdown activates the Wnt pathway, downregulates E-cadherin expression, and promotes its degradation. Conversely, ANK3-TV4 overexpression inhibited the Wnt pathway, upregulated E-cadherin protein expression, and inhibited its degradation (Fig. 6g,h). Finally, we analyzed the correlation between E-cadherin and ANK3 proteins in clinical samples from the Clinical Proteomic Tumor Analysis Consortium (CPTAC) database of The Cancer Genome Atlas (TCGA) and found that E-cadherin protein positively correlated with ANK3 protein in both liver cancer and paracancer samples, which was consistent with our previous conclusions (Fig. 6i).

3.6 Knockdown of RBM8A Promoted RS of ANK3-TV4

Multiple annotated RS-exons in human mRNAs can be attributed to the inhibition of RS by EJC. The EJC is generally composed of core EJC factors, including *eIF4A3*, *MAGOH*, and *RBM8A*, and peripheral factors such as *PNN* and *RNPS1* [17]. Screening of candidate factors in clinical HCC samples revealed that *RBM8A* was the sole factor significantly overexpressed (Fig. 8a,b), consistent with publicly available data (Fig. 8c). Kaplan-Meier analysis of overall survival in the TCGA liver cancer cohort (n = 182) demonstrated a significant reduction in survival time for patients with high *RBM8A* expression (Fig. 8d). Elevated *RBM8A* expression was significantly correlated with reduced disease-free survival in HCC patients from the TCGA-LIHC cohort (Fig. 8e), underscoring its negative impact on patient prognosis.



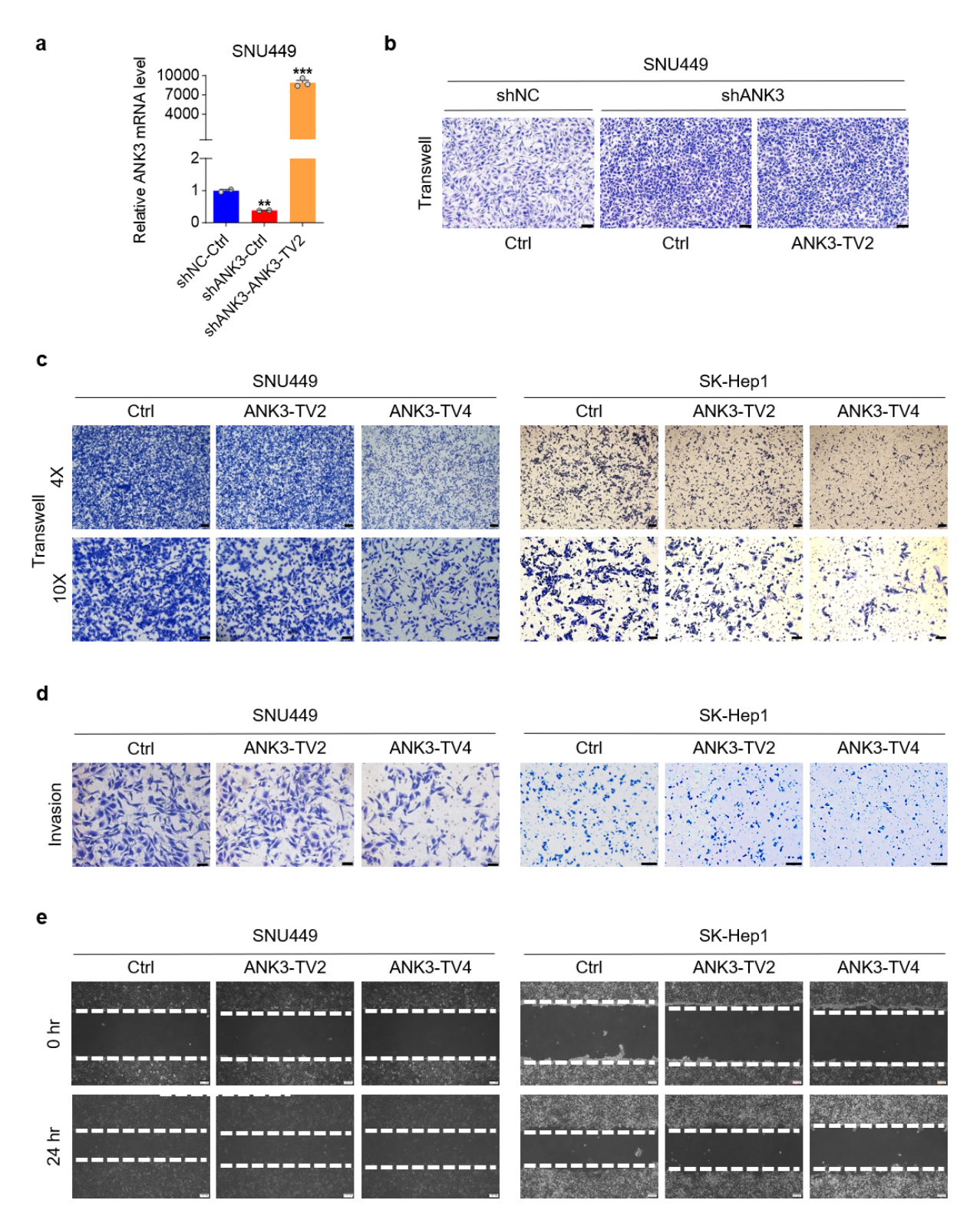


Fig. 4. Ankyrin repeats of *ANK3* **are critical in cell migration.** (a) *ANK3* mRNA expression in SNU449 cells with stable ANK3-total knockdown, following transfection with an empty vector (Ctrl) or an *ANK3-TV2* overexpression vector. (b) Transwell assay of *ANK3-TV2* overexpression in stable cell lines with *ANK3*-total knockdown. (c) Transwell assay of SNU449 (left) or SK-Hep1 (right) cells transfected with ctrl (Empty Vector) or *ANK3-TV2/ANK3-TV4* overexpression vectors. (d) Invasion assay of SNU449 (left) or SK-Hep1 (right) cells transfected with ctrl (Empty Vector) or *ANK3-TV2/ANK3-TV4* overexpression vectors. (e) Wound-healing assay of SNU449 (left) or SK-Hep1 cells (right) transfected with ctrl (Empty Vector) or *ANK3-TV2/ANK3-TV4* overexpression vectors. Scale bar: 100 μm (b), 200 μm (c 4×), 100 μm (c 10×), 100 μm (d), 200 μm (e). Data are shown as mean ± SEM, Student's paired *t* test, **p < 0.01, ***p < 0.001.

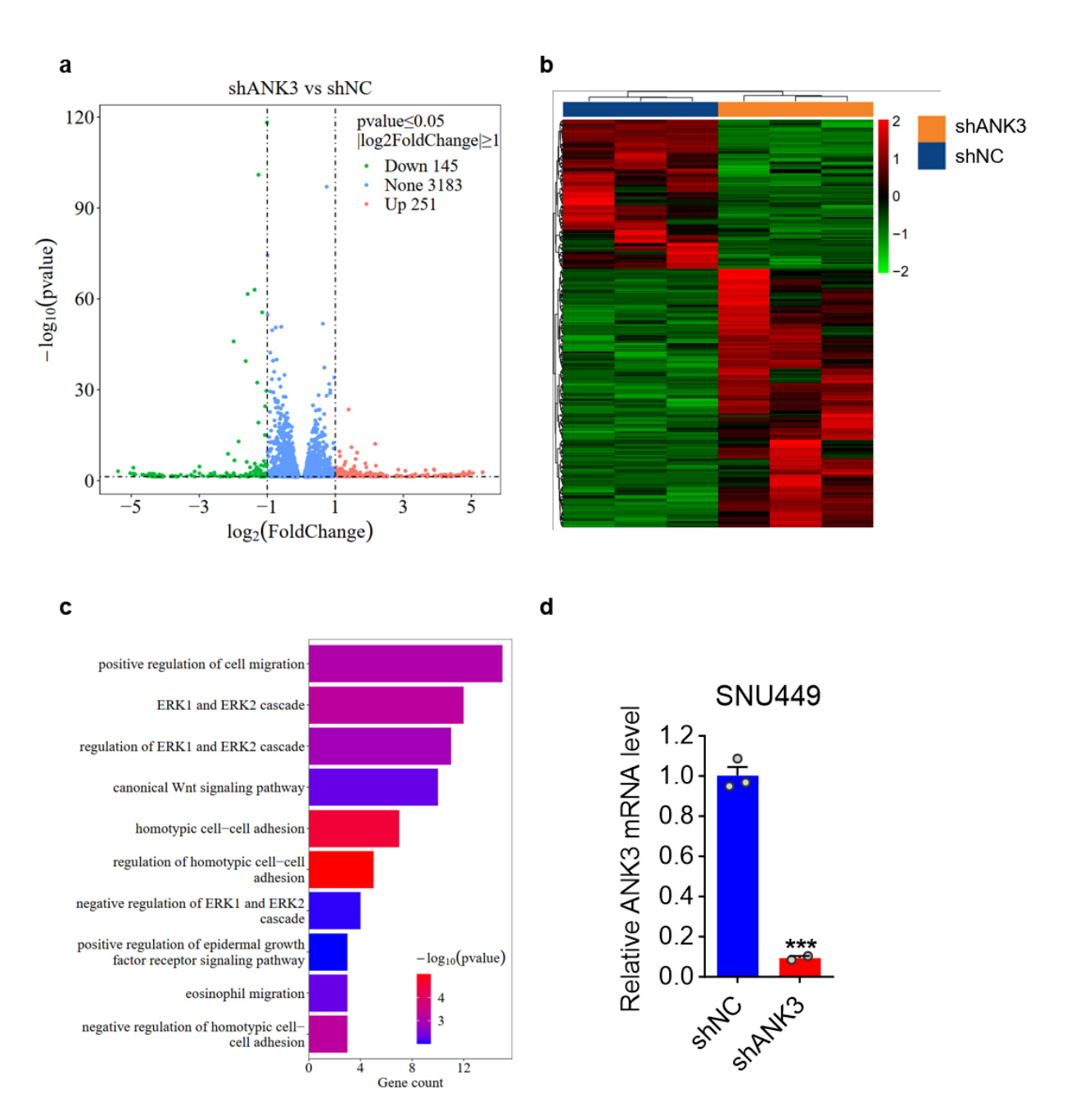


Fig. 5. Enrichment analysis of differentially expressed protein-coding genes in SNU449 cells with stable ANK3 knockdown. (a) A volcano plot visualization of the data. The X-axis represents the magnitude of expression change (\log_2 fold change), while the Y-axis indicates the statistical significance ($-\log_{10} p$ -value) of that change. Genes are highlighted as down-regulated (green), up-regulated (red), or unchanged (blue). (b) Cluster heat maps: Each column represents a sample, and each group has 3 biologically duplicated samples. Each line represents a protein-coding gene. Fragments Per Kilobase Million (FPKM) values were used for clustering, with red representing high-expression genes and green representing low-expression genes, and the darker the color, the greater the degree of up-regulation or down-regulation. (c) Gene Ontology Enrichment Analysis (GO): The vertical axis is the name of the GO pathway, and the horizontal axis represents the number of genes enriched into that pathway. The darker the color, the smaller the p value, indicating that the enrichment significance of differentially expressed genes in this pathway is more reliable. (d) qRT-PCR analysis of ANK3 expression in SNU449 cells infected with shNC or shANK3 lentivirus. Data are presented as mean \pm SEM, ***p < 0.001 (Student's paired t test).

We next investigated the functional contribution of *RBM8A* to liver tumorigenesis. Functional interrogation of *RBM8A* in liver tumorigenesis revealed that its siRNA-

mediated knockdown attenuated the proliferation of SK-Hep1 and SNU449 cells (Fig. 8h), and markedly impaired the migration and invasion of SK-Hep1 cells (Fig. 8f).



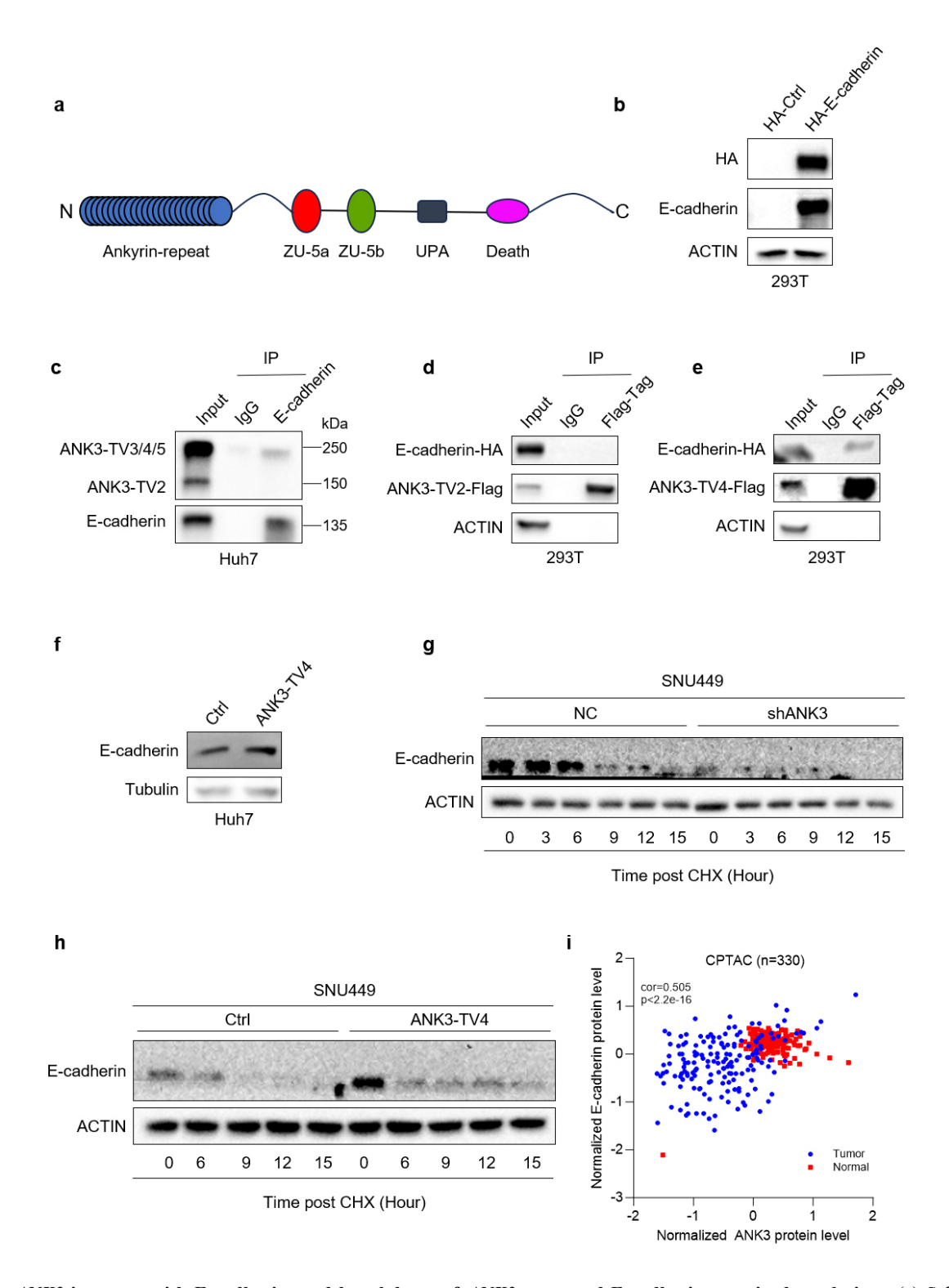


Fig. 6. *ANK3* interacts with E-cadherin, and knockdown of *ANK3* promoted E-cadherin protein degradation. (a) Schematic diagram of the *ANK3* domain. (b) Validation of HA-tagged control and E-cadherin plasmid expression in 293T cells by WB. (c) Endogenous interaction between ANK3 and E-cadherin in Huh7 cells, confirmed by co-immunoprecipitation. (d,e) Exogenous interaction of E-cadherin with ANK3-TV2 (d) or ANK3-TV4 (e) in 293T cells, assessed by co-immunoprecipitation. (f) Overexpression of *ANK3-TV4* significantly upregulated E-cadherin. (g) Knockdown of *ANK3* promoted E-cadherin protein degradation. (h) Overexpression of *ANK3-TV4* inhibited E-cadherin protein degradation. (i) E-cadherin protein and ANK3 protein were positively correlated in HCC in the CPTAC database.

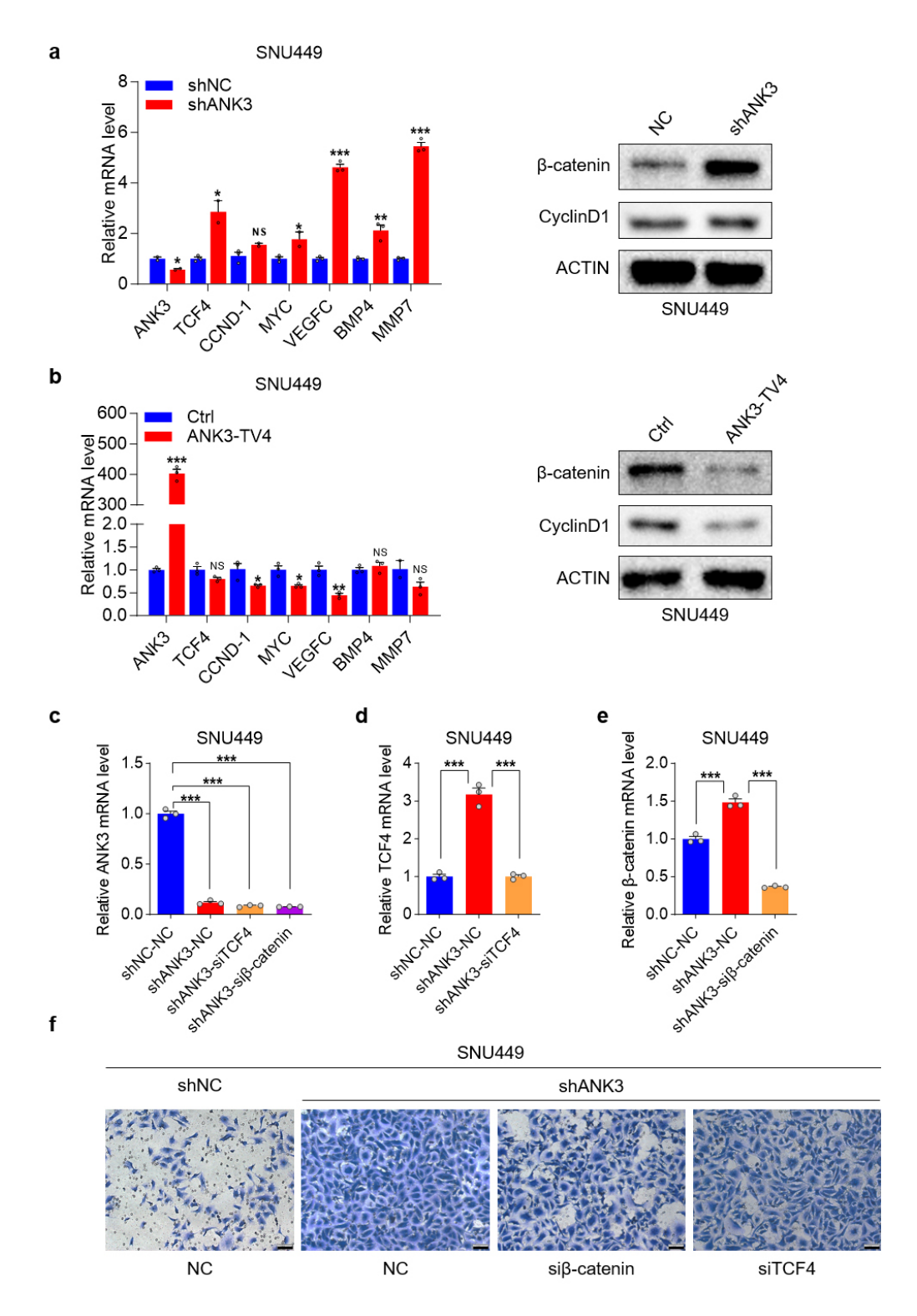


Fig. 7. Knockdown of *ANK3* **activates the Wnt pathway.** (a) qRT-PCR and WB analysis of Wnt pathway factor expression upon *ANK3* knockdown in SNU449 cells. (b) qRT-PCR and WB analysis of Wnt pathway components in response to *ANK3-TV4* overexpression in SNU449 cells. (c) qRT-PCR analysis of *ANK3* expression in response to transient $TCF4/\beta$ -catenin knockdown in stable *ANK3*-knockdown cell lines. (d) TCF4 expression level was detected following transient knockdown of TCF4 in stable cell lines with ANK3-total knockdown. (e) The expression level of *β*-catenin was detected after transient knockdown of *β*-catenin in stable cell lines with *ANK3*-total knockdown. (f) Transwell assay after transient knockdown of $TCF4/\beta$ -catenin in stable cell lines with *ANK3*-total knockdown. Scale bar: 100 μm. Data are presented as mean ± SEM, NS: p > 0.05, *p < 0.05, *p < 0.01, ***p < 0.001 (Student's paired p < 0.001) test).



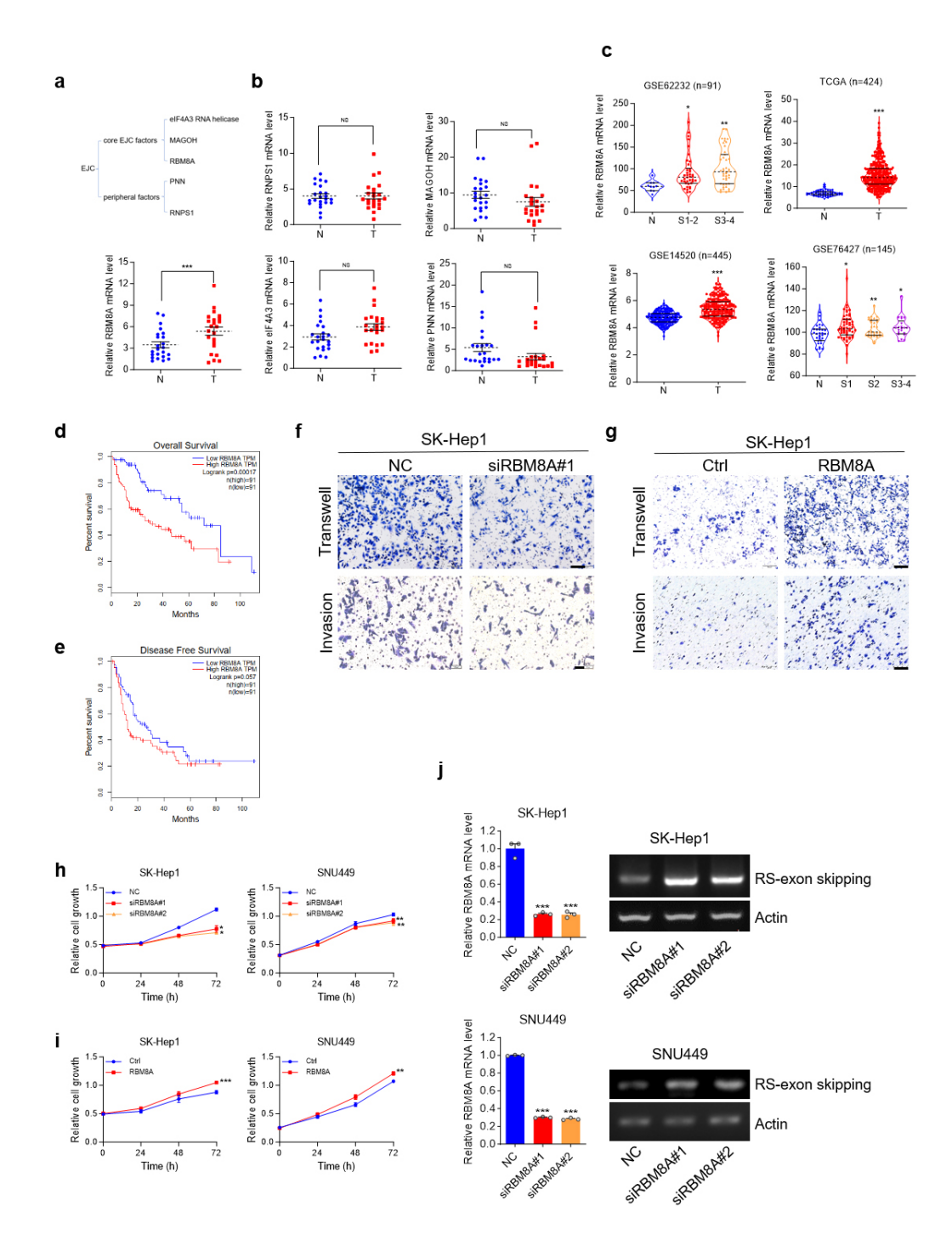


Fig. 8. RBMBA is upregulated in HCC. Knockdown of RBM8A inhibits the proliferation and metastasis of HCC cells, and knockdown of RBM8A promotes RS of ANK3-TV4. (a) Schematic of exon junction complex (EJC). (b) qRT-PCR analysis of EJC factors identifies RBM8A as the sole significantly upregulated member in HCC. (c) RBM8A mRNA levels in HCC and normal livers from published cohorts. (d) Kaplan-Meier analysis of overall survival data from TCGA cohort (n = 182), stratified by RBM8A expression. (e) Kaplan-Meier analysis of disease free survival in the TCGA-LIHC cohort (n = 182). (f) Impact of RBM8A depletion on the migratory and invasive capacity of SK-Hep1 cells. (g) Effect of RBM8A overexpression on the migratory and invasive capacity of SK-Hep1 cells. (h) MTS analysis of SK-Hep1 (left) and SNU449 (right) cells transfected with NC or siRBM8A. (i) MTS analysis of SK-Hep1 (left) and SNU449 (right) cells transfected with ctrl (Empty Vector) or RBM8A overexpression vector. (j) The semi-quantitative RT-PCR proved that knocking down RBM8A promotes RS of ANK3-TV4 in SK-Hep1 or SNU449 cells. Actin: 25 cycles; ANK3-TV4 with RS-exon skipping: 42 cycles. Scale bar: 100 μm. Data are presented as mean ± SEM, NS: p > 0.05, *p < 0.05, *p < 0.01, ***p < 0.001 (Student's paired p < 0.001 test).

Conversely, *RBM8A* overexpression enhanced these malignant properties, including migration, invasion, and growth (Fig. 8g,i). Collectively, these findings establish *RBM8A* as a promoter of HCC cell proliferation, migration, and invasion *in vitro*.

The role of *RBM8A* in modulating the RS of *ANK3-TV4* was assessed. Transcripts with RS-exon skipping were quantified using primers crossing the first and second exons of *ANK3-TV4*. The data indicate that reducing *RBM8A* levels promotes RS of *ANK3-TV4* (Fig. 8j), which promoted the jump of the RS-exon, reducing the NMD of *ANK3-TV4*. Thus, normal functional *ANK3-TV4* was upregulated.

4. Discussion

In 1998, Hatton et al. [32] first discovered the RS in Drosophila melanogaster *Ubx* and identified a new splicing site between the first and second exons of the Ubx gene. Researchers have conducted in-depth studies on the Ubx gene and found that the first intron of the gene is 73 kb long, and the removal of the intron involves three splicing steps [33]. In 2015, Sibley et al. [16] conducted deep RNA sequencing of vertebrate neurons and found that RS phenomena are widespread in vertebrate neurons, including in genes such as ANK3 and CADM2. Emmett [34] found that in the human brain tissue, seven genes associated with RS are closely related to neurological diseases. Given the established link between aberrant long-gene expression and neurological disorders [35-37], it is plausible that mutations or deletions at RS sites constitute another mechanism for human genetic diseases [16]. RS events, observed in diverse cell types including neurons [34] and endodermal cells [38], are associated with a spectrum of human diseases spanning neurological (e.g., Parkinson's) and circulatory (e.g., retinal sclerosis, hypertension) disorders [39]. In addition, Srndic [40] detected over 12,000 RS events in multiple human tissues and found that RS might play a role in nonsense-mediated RNA decay.

ANK3 was originally identified in the axonal initial segment and nodes of Ranvier [41,42]. It has been extensively characterized and is now recognized as an established risk gene for several neuropsychiatric disorders, including bipolar disorder, schizophrenia, and autism spectrum disorder [21,43–45]. A relevant study has reported that ANK3 undergoes RS [16], but did not indicate the transcript in which the RS is present. ANK3 is perversely expressed in various human cancers; however, the underlying mechanism remains unclear. Currently, only studies have reported the function of ANK3 in prostate cancer [26], and colorectal cancer [46].

Referring to the study by Blazquez *et al.* [17], who found that the EJC suppressed hundreds of annotated RS, mainly constitutive RS-exons, and they investigated the role of EJC in regulating the RS of *CADM2*, mainly by RT-PCR. Given this context, we sought to determine whether the EJC, particularly its key components, regulates *ANK3*

in HCC. Systematic examination of EJC factors in clinical HCC samples revealed RBM8A as the sole significantly upregulated member. Subsequent functional characterization confirmed the oncogenic properties of RBM8A. Therefore, we explored the effect of RBM8A on ANK3 RS. However, we did not successfully detect RS by RT-PCR using the primers used in the study by Sibley et al. [16]; thus, we redesigned the primers to specifically detect the expression of RS transcripts by semi-quantitative PCR. Knockdown of RBM8A significantly promoted the RS of ANK3-TV4, which promoted a jump in the RS-exon, reducing the NMD of ANK3-TV4. Thus, normally functional ANK3-TV4 is upregulated, inhibiting cell migration. Of course, RBM8A's regulation on the RS of the ANK3-TV4 is only slight, and this regulatory process must involve many other factors and more complex pathways. Our study merely preliminarily links RS to HCC. However, it is not yet clear whether the anti-metastasis effect of RBM8A depletion is specifically mediated by ANK3-TV4 RS.

Durak et al. [29] demonstrated that ANK3 regulates canonical Wnt signaling by modulating the subcellular localization and availability of β -catenin in proliferating cells. They found that ANK3 deficiency disrupts the β catenin/E-cadherin interaction, leading to increased nuclear translocation of β -catenin, which in turn enhances Wnt signaling and promotes neural progenitor cell proliferation. However, the study did not address the subsequent fate of E-cadherin. Our results indicated that ANK3 knockdown downregulates E-cadherin, promotes E-cadherin degradation, and activates the Wnt pathway, thus promoting HCC metastasis. Our study did not compare the Wnt inhibition mediated by ANK3 with other reported Wnt regulators in HCC (such as AXIN2, APC), nor did it test whether ANK3 affects EMT markers (such as N-cadherin, vimentin, Snail), which are the key downstream effects of E-cadherin regulation. This is one of the deficiencies of this study. This study initially indicates that ANK3 is involved in regulating the Wnt signaling pathway. The mechanism by which it participates in HCC pathogenesis by regulating the Wnt pathway requires further elucidation.

The growing recognition of introns as critical regulators of gene expression, driven by advances in RNA sequencing, highlights the importance of deciphering RS in this process. HCC is the third most common cause of cancer mortality worldwide [47], creating an urgent need to define its molecular drivers, particularly for metastasis [26]. Investigating RS may therefore yield novel therapeutic targets for this lethal malignancy. We studied the effects of ANK3 on HCC development via its regulation by RS. This study only explored the regulation of *RBM8A* on the RS of *ANK3-TV4* at the mRNA level, but there was no discussion on the level of *ANK3* protein. Therefore, it is difficult to link it with the downstream mechanism of *ANK3* regulation. In addition, the puzzling thing is that the expression pattern of the protein near 250 kDa (*ANK3-TV3/4/5*) in HCC is un-



certain, which is not completely consistent with the tumor suppressive function of *ANK3*. Therefore, more complex regulatory mechanisms at the protein level need to be explored. Further *in vivo* experiments are required to assess the antitumor efficacy of *ANK3*.

5. Conclusions

In summary, we found that *ANK3* was downregulated in HCC and inhibited HCC metastasis, confirming that RS exists in *ANK3-TV4* and that RS is weakened in HCC. *RBM8A*, a core EJC factor, regulates the RS of *ANK3-TV4*. Mechanistically, *ANK3* regulates HCC progression by simultaneously controlling the expression of E-cadherin and the Wnt signaling pathway. Our study on RS regulation of *ANK3* is superficial, but it provides a new idea for introns to regulate gene expression and participate in disease, and an in-depth study of RS, *ANK3*, and EJC may pave the way for developing targeted therapies against HCC.

Availability of Data and Materials

The datasets used and analyzed during the current study are available from the corresponding author on reasonable request.

Author Contributions

YG, XF and YT designed the research study. YG performed the research. YG analyzed the data. YG wrote the manuscript. YT provided help on the revision of the article. All authors contributed to editorial changes in the manuscript. All authors read and approved the final manuscript. All authors have participated sufficiently in the work and agreed to be accountable for all aspects of the work.

Ethics Approval and Consent to Participate

The study was conducted in accordance with the Declaration of Helsinki. The research protocol was approved by the Ethics Committee of Institutional Review Committee of West China Hospital of Sichuan University (Ethic Approval Number: 2020, no. 196) and all of the participants provided signed informed consent.

Acknowledgment

Not applicable.

Funding

This research received no external funding.

Conflict of Interest

The authors declare no conflict of interest.

Supplementary Material

Supplementary material associated with this article can be found, in the online version, at https://doi.org/10.31083/FBL46013.

References

- [1] Llovet JM, Pinyol R, Yarchoan M, Singal AG, Marron TU, Schwartz M, et al. Adjuvant and neoadjuvant immunotherapies in hepatocellular carcinoma. Nature Reviews. Clinical Oncology. 2024; 21: 294–311. https://doi.org/10.1038/ s41571-024-00868-0.
- [2] Yeo YH, Abdelmalek M, Khan S, Moylan CA, Rodriquez L, Villanueva A, et al. Current and emerging strategies for the prevention of hepatocellular carcinoma. Nature Reviews. Gastroenterology & Hepatology. 2025; 22: 173–190. https://doi.org/10. 1038/s41575-024-01021-z.
- [3] Li S, Hu Z, Zhao Y, Huang S, He X. Transcriptome-Wide Analysis Reveals the Landscape of Aberrant Alternative Splicing Events in Liver Cancer. Hepatology (Baltimore, Md.). 2019; 69: 359–375. https://doi.org/10.1002/hep.30158.
- [4] Lee SE, Alcedo KP, Kim HJ, Snider NT. Alternative Splicing in Hepatocellular Carcinoma. Cellular and Molecular Gastroenterology and Hepatology. 2020; 10: 699–712. https://doi.org/10. 1016/j.jcmgh.2020.04.018.
- [5] Jobbins AM, Yu S, Paterson HAB, Maude H, Kefala-Stavridi A, Speck C, et al. Pre-RNA splicing in metabolic homeostasis and liver disease. Trends in Endocrinology and Metabolism: TEM. 2023; 34: 823–837. https://doi.org/10.1016/j.tem.2023.08.007.
- [6] Xu K, Wu T, Xia P, Chen X, Yuan Y. Alternative splicing: a bridge connecting NAFLD and HCC. Trends in Molecular Medicine. 2023; 29: 859–872. https://doi.org/10.1016/j.molm ed.2023.07.001.
- [7] Wu Q, Liao R, Miao C, Hasnat M, Li L, Sun L, et al. Oncofetal SNRPE promotes HCC tumorigenesis by regulating the FGFR4 expression through alternative splicing. British Journal of Cancer. 2024; 131: 77–89. https://doi.org/10.1038/s41416-024-02689-5.
- [8] Wang H, Qian D, Wang J, Liu Y, Luo W, Zhang H, et al. HnRNPR-mediated UPF3B mRNA splicing drives hepatocellular carcinoma metastasis. Journal of Advanced Research. 2025; 68: 257–270. https://doi.org/10.1016/j.jare.2024.02.010.
- [9] Nie D, Tang X, Deng H, Yang X, Tao J, Xu F, et al. Metabolic Enzyme SLC27A5 Regulates PIP4K2A pre-mRNA Splicing as a Noncanonical Mechanism to Suppress Hepatocellular Carcinoma Metastasis. Advanced Science (Weinheim, Baden-Wurttemberg, Germany). 2024; 11: e2305374. https://doi.org/ 10.1002/advs.202305374.
- [10] Yan Q, Fang X, Liu X, Guo S, Chen S, Luo M, et al. Loss of ESRP2 Activates TAK1-MAPK Signaling through the Fetal RNA-Splicing Program to Promote Hepatocellular Carcinoma Progression. Advanced science (Weinheim, Baden-Wurttemberg, Germany). 2024; 11: e2305653. https://doi.org/ 10.1002/advs.202305653.
- [11] Do HTT, Shanak S, Barghash A, Helms V. Differential exon usage of developmental genes is associated with deregulated epigenetic marks. Scientific Reports. 2023; 13: 12256. https: //doi.org/10.1038/s41598-023-38879-z.
- [12] Bradley RK, Anczuków O. RNA splicing dysregulation and the hallmarks of cancer. Nature Reviews. Cancer. 2023; 23: 135– 155. https://doi.org/10.1038/s41568-022-00541-7.
- [13] Li D, Yu W, Lai M. Towards understandings of serine/argininerich splicing factors. Acta Pharmaceutica Sinica. B. 2023; 13: 3181–3207. https://doi.org/10.1016/j.apsb.2023.05.022.
- [14] Sinitcyn P, Richards AL, Weatheritt RJ, Brademan DR, Marx



- H, Shishkova E, *et al.* Global detection of human variants and isoforms by deep proteome sequencing. Nature Biotechnology. 2023; 41: 1776–1786. https://doi.org/10.1038/s41587-023-01714-x.
- [15] Ule J, Blencowe BJ. Alternative Splicing Regulatory Networks: Functions, Mechanisms, and Evolution. Molecular Cell. 2019; 76: 329–345. https://doi.org/10.1016/j.molcel.2019.09.017.
- [16] Sibley CR, Emmett W, Blazquez L, Faro A, Haberman N, Briese M, et al. Recursive splicing in long vertebrate genes. Nature. 2015; 521: 371–375. https://doi.org/10.1038/nature14466.
- [17] Blazquez L, Emmett W, Faraway R, Pineda JMB, Bajew S, Gohr A, et al. Exon Junction Complex Shapes the Transcriptome by Repressing Recursive Splicing. Molecular Cell. 2018; 72: 496–509.e9. https://doi.org/10.1016/j.molcel.2018.09.033.
- [18] Le Hir H, Saulière J, Wang Z. The exon junction complex as a node of post-transcriptional networks. Nature Reviews. Molecular Cell Biology. 2016; 17: 41–54. https://doi.org/10.1038/nr m.2015.7.
- [19] Tang Y, He Y, Zhang P, Wang J, Fan C, Yang L, et al. LncRNAs regulate the cytoskeleton and related Rho/ROCK signaling in cancer metastasis. Molecular Cancer. 2018; 17: 77. https://doi. org/10.1186/s12943-018-0825-x.
- [20] Bennett V, Chen L. Ankyrins and cellular targeting of diverse membrane proteins to physiological sites. Current Opinion in Cell Biology. 2001; 13: 61–67. https://doi.org/10.1016/s0955-0674(00)00175-7.
- [21] Wang T, Abou-Ouf H, Hegazy SA, Alshalalfa M, Stoletov K, Lewis J, et al. Ankyrin G expression is associated with androgen receptor stability, invasiveness, and lethal outcome in prostate cancer patients. Journal of Molecular Medicine (Berlin, Germany). 2016; 94: 1411–1422. https://doi.org/10.1007/s00109-016-1458-4.
- [22] Schwartz S, Wilson SJ, Hale TK, Fitzsimons HL. Ankyrin2 is essential for neuronal morphogenesis and long-term courtship memory in Drosophila. Molecular Brain. 2023; 16: 42. https://doi.org/10.1186/s13041-023-01026-w.
- [23] Hughes T, Hansson L, Sønderby IE, Athanasiu L, Zuber V, Tesli M, et al. A Loss-of-Function Variant in a Minor Isoform of ANK3 Protects Against Bipolar Disorder and Schizophrenia. Biological Psychiatry. 2016; 80: 323–330. https://doi.org/ 10.1016/j.biopsych.2015.09.021.
- [24] Furia F, Levy AM, Theunis M, Bamshad MJ, Bartos MN, Bijlsma EK, et al. The phenotypic and genotypic spectrum of individuals with mono- or biallelic ANK3 variants. Clinical Genetics. 2024; 106: 574–584. https://doi.org/10.1111/cge.14587.
- [25] Fu X, Meng Z, Liang W, Tian Y, Wang X, Han W, et al. miR-26a enhances miRNA biogenesis by targeting Lin28B and Zcchc11 to suppress tumor growth and metastasis. Oncogene. 2014; 33: 4296–4306. https://doi.org/10.1038/onc.2013.385.
- [26] Ma M, Xu H, Liu G, Wu J, Li C, Wang X, et al. Metabolism-induced tumor activator 1 (MITA1), an Energy Stress-Inducible Long Noncoding RNA, Promotes Hepatocellular Carcinoma Metastasis. Hepatology (Baltimore, Md.). 2019; 70: 215–230. https://doi.org/10.1002/hep.30602.
- [27] Fu X, Dong B, Tian Y, Lefebvre P, Meng Z, Wang X, et al. MicroRNA-26a regulates insulin sensitivity and metabolism of glucose and lipids. The Journal of Clinical Investigation. 2015; 125: 2497–2509. https://doi.org/10.1172/JC175438.
- [28] Jenkins PM, Kim N, Jones SL, Tseng WC, Svitkina TM, Yin HH, et al. Giant ankyrin-G: a critical innovation in vertebrate evolution of fast and integrated neuronal signaling. Proceedings of the National Academy of Sciences of the United States of America. 2015; 112: 957–964. https://doi.org/10.1073/pnas.1416544112.
- [29] Durak O, de Anda FC, Singh KK, Leussis MP, Petryshen TL, Sklar P, et al. Ankyrin-G regulates neurogenesis and Wnt signaling by altering the subcellular localization of β-catenin. Molec-

- ular Psychiatry. 2015; 20: 388–397. https://doi.org/10.1038/mp.2014.42.
- [30] Li Y, Liu C, Zhang X, Huang X, Liang S, Xing F, et al. CCT5 induces epithelial-mesenchymal transition to promote gastric cancer lymph node metastasis by activating the Wnt/β-catenin signalling pathway. British Journal of Cancer. 2022; 126: 1684–1694. https://doi.org/10.1038/s41416-022-01747-0.
- [31] Tu W, Gong J, Zhou Z, Tian D, Wang Z. TCF4 enhances hepatic metastasis of colorectal cancer by regulating tumor-associated macrophage via CCL2/CCR2 signaling. Cell Death & Disease. 2021; 12: 882. https://doi.org/10.1038/s41419-021-04166-w.
- [32] Hatton AR, Subramaniam V, Lopez AJ. Generation of alternative Ultrabithorax isoforms and stepwise removal of a large intron by resplicing at exon-exon junctions. Molecular Cell. 1998; 2: 787–796. https://doi.org/10.1016/s1097-2765(00)80293-2.
- [33] Burnette JM, Miyamoto-Sato E, Schaub MA, Conklin J, Lopez AJ. Subdivision of large introns in Drosophila by recursive splicing at nonexonic elements. Genetics. 2005; 170: 661–674. https://doi.org/10.1534/genetics.104.039701.
- [34] Emmett WA. Computational identification of regulatory features affecting splicing in the human brain [Doctoral thesis]. UCL. 2016.
- [35] Lagier-Tourenne C, Polymenidou M, Hutt KR, Vu AQ, Baughn M, Huelga SC, et al. Divergent roles of ALS-linked proteins FUS/TLS and TDP-43 intersect in processing long pre-mRNAs. Nature Neuroscience. 2012; 15: 1488–1497. https://doi.org/10.1038/nn.3230.
- [36] Polymenidou M, Lagier-Tourenne C, Hutt KR, Huelga SC, Moran J, Liang TY, et al. Long pre-mRNA depletion and RNA missplicing contribute to neuronal vulnerability from loss of TDP-43. Nature Neuroscience. 2011; 14: 459–468. https://do i.org/10.1038/nn.2779.
- [37] King IF, Yandava CN, Mabb AM, Hsiao JS, Huang HS, Pearson BL, et al. Topoisomerases facilitate transcription of long genes linked to autism. Nature. 2013; 501: 58–62. https://doi.org/10.1038/nature12504.
- [38] Kelly S, Georgomanolis T, Zirkel A, Diermeier S, O'Reilly D, Murphy S, *et al.* Splicing of many human genes involves sites embedded within introns. Nucleic Acids Research. 2015; 43: 4721–4732. https://doi.org/10.1093/nar/gkv386.
- [39] Georgomanolis T, Sofiadis K, Papantonis A. Cutting a Long Intron Short: Recursive Splicing and Its Implications. Frontiers in Physiology. 2016; 7: 598. https://doi.org/10.3389/fphys.2016. 00598.
- [40] Srndic I. Experimental verification and functional exploration of intrasplicing [Master's thesis]. Wien, Austria: Universität Wien. 2016
- [41] Grubb MS, Burrone J. Building and maintaining the axon initial segment. Current Opinion in Neurobiology. 2010; 20: 481–488. https://doi.org/10.1016/j.conb.2010.04.012.
- [42] Lambert S, Davis JQ, Bennett V. Morphogenesis of the node of Ranvier: co-clusters of ankyrin and ankyrin-binding integral proteins define early developmental intermediates. The Journal of Neuroscience: the Official Journal of the Society for Neuroscience. 1997; 17: 7025–7036. https://doi.org/10.1523/JNEU ROSCI.17-18-07025.1997.
- [43] Ferreira MAR, O'Donovan MC, Meng YA, Jones IR, Ruderfer DM, Jones L, et al. Collaborative genome-wide association analysis supports a role for ANK3 and CACNA1C in bipolar disorder. Nature Genetics. 2008; 40: 1056–1058. https://doi.org/10.1038/ng.209.
- [44] Smith EN, Bloss CS, Badner JA, Barrett T, Belmonte PL, Berrettini W, et al. Genome-wide association study of bipolar disorder in European American and African American individuals. Molecular Psychiatry. 2009; 14: 755–763. https://doi.org/10.1038/mp.2009.43.



- [45] Pandey A, Davis NA, White BC, Pajewski NM, Savitz J, Drevets WC, et al. Epistasis network centrality analysis yields pathway replication across two GWAS cohorts for bipolar disorder. Translational Psychiatry. 2012; 2: e154. https://doi.org/10.1038/ tp.2012.80.
- [46] Zhang N, Yue W, Jiao B, Cheng D, Wang J, Liang F, *et al.* Unveiling prognostic value of JAK/STAT signaling pathway related genes in colorectal cancer: a study of Mendelian random-
- ization analysis. Infectious Agents and Cancer. 2025; 20: 9. https://doi.org/10.1186/s13027-025-00640-8.
- [47] Bray F, Ferlay J, Soerjomataram I, Siegel RL, Torre LA, Jemal A. Global cancer statistics 2018: GLOBOCAN estimates of incidence and mortality worldwide for 36 cancers in 185 countries. CA: A Cancer Journal for Clinicians. 2018; 68: 394–424. https://doi.org/10.3322/caac.21492.

